THE JOURNAL OF PHYSICAL CHEMISTRY B

Article

Cite This: J. Phys. Chem. B 2018, 122, 9264−9273

pubs.acs.org/JPCB

Disorder Foreshadows Order in Colloidal Cubes

Abhishek K. Sharma and Fernando A. Escobedo*

Robert Frederick Smith School of Chemical and Biomolecular Engineering, Cornell University, Ithaca, New York 14853, United States

Supporting Information

ABSTRACT: Monte Carlo simulations are used to investigate the mechanism of the disorder-to-order phase transition for a bulk system of colloidal hard cubes. It is observed that the structure of the ordered state is foreshadowed in the disordered state through multiple spontaneously occurring ordered domains. Such domains arise due to the entropic preference for local facet alignment between particles and occur transiently and sparsely throughout the system even in the stable isotropic phase. At pressures (and degrees of supersaturation) where the isotropic phase becomes marginally metastable, a classical nucleation process is never observed; instead, the ordered domains increase in number and size, eventually reaching a critical point where they percolate the entire system and spontaneously consolidate to form the ordered phase. The critical number of particles and the per particle free-energy barrier both decrease with pressure. Using the total number of locally ordered particles as a global order parameter, it is predicted that for large systems the ordering transition would only be spontaneous above a critical pressure. Finally, a test designed to probe the ability of the system to favor a single monodomain solid from initially misaligned-ordered domains, reveals that an active interdomain zone mediates the concerted reorientation of particles.

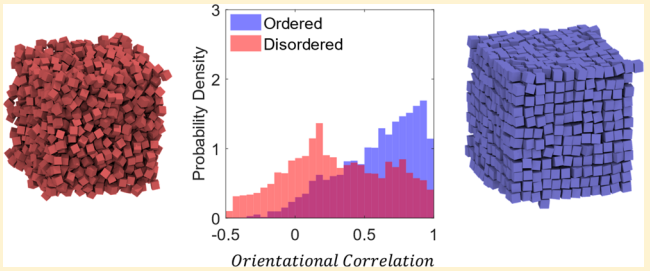

1. INTRODUCTION

Microscopic colloidal particles can self-assemble into complex mesoscale structures[1] whose characteristics are dictated by individual features of the particles, such as size, shape, and specific interparticle interactions.[2] With recent advances in our ability to synthesize nanoparticles with precise control over those individual features, a concurrent interest has bloomed to understand the design principles to engineer desired behaviors out of such customizable components.[3] Not only can such a design be of practical importance but it can also reveal general principles about the way how naturally occurring systems self-assemble into exquisitely complex microstructures.[4]

It has long been known that entropic effects[5] alone can result in the self-assembly of hard spherical particles into a close-packed lattice.[6] Oblong hard particles and rods, which possess additional orientational degrees of freedom, result in the formation of different ordered states, such as nematic phases with aligned particles, where the loss of orientational entropy is compensated by a gain in translational entropy.[7] A further level of particle shape complexity has been explored by considering faceted particles, such as polyhedra,[8,9] where their additional orientational degrees of freedom can lead to the formation of different types of crystals and mesophases (thus called for they are neither completely disordered (isotropic) nor completely ordered (crystal)). To control the emergence of these phases in polyhedral systems[10,11] it is important to study and characterize not only their thermodynamic behavior but also the mechanisms underlying disorder-to-order phase transitions. Similar to hard spheres,[12,13] the transitions involved are often first-order transitions,[14] comprising nucleation and growth of the incipient phase from a metastable mother phase. Recent studies[15−17] have revealed several design rules for engineering the particle shape to control the ease of self-assembly. For example, it was observed[15] that for several polyhedra with small asphericity and high rotational symmetry, translationally ordered rotator phases nucleate from the disordered state with a smaller free-energy barrier than that observed for hard spheres at a comparable degree of supersaturation (DSS). This trend was attributed to the presence of productive correlations between local orientational order and translational order, which catalyze the isotropic-to-rotator phase transition. Recently, it was reported[16] that even though similar local fluctuations in orientational order are ubiquitous for other polyhedral shapes, their effect is only catalytic when the final-ordered phase comprises configurations with extensive facet alignment between neighboring particles. This is because the excluded volume for a pair of neighbor faceted particles tends to be minimized, and the local packing entropy maximized, if their facets align. Because such high local entropy configurations spontaneously occur in the disordered phase, systems whose solid phase exhibits high facet alignment (like truncated octahedra and rhombic dodecahedra) will tend to have lower transition free-energy barriers than systems whose solid phase exhibits no such facet alignment

Received: June 28, 2018
Revised: August 27, 2018
Published: September 6, 2018

DOI: 10.1021/acs.jpcb.8b06207
J. Phys. Chem. B 2018, 122, 9264−9273

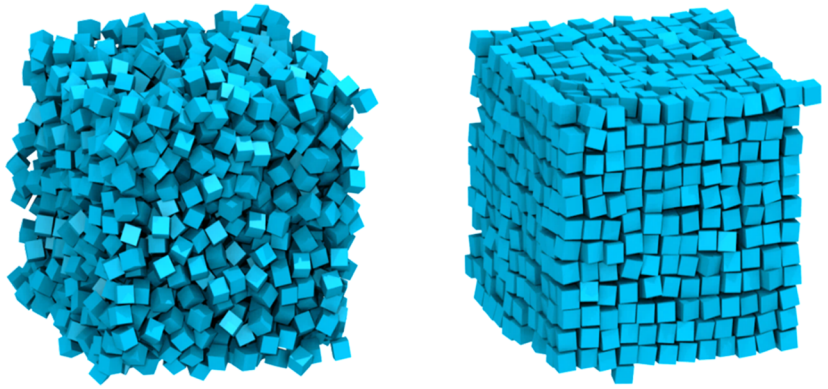

Figure 1. Sample snapshots of the disordered (left) and ordered (right) phases in hard cubes near the disorder−order transition.

(like octahedra). In fact, the latter systems will even tend to have higher transition free-energy barriers than hard spheres since the spontaneously occurring facet-aligned configurations in the isotropic phase are counterproductive toward forming the solid phase. Thus, the extent of "coherence" between local vs global packing tendencies of such polyhedral systems during phase transition can lead to facilitated or impeded self-assembly.

In this work, we explore the disorder-to-order transition mechanism of hard cubes, an archetypal case of a system that exhibits strong coherence between local and global packing tendencies during ordering. Because hard cubes have equal facets and the ordered phase entails perfect facet alignment, it is expected that cubes would be one of the easiest systems to self-assemble. Cubes have been shown to possess an interesting phase behavior (see Figure 1) with a disordered liquid phase at low pressure, a simple cubic crystal at high pressures, and a cubic mesophase in between that merges continuously with the crystal phase.[8] This cubic mesophase could be seen as a state where the crystal phase contains a high concentration of mobile vacancies; in fact such vacancies have been described as key contributors to the crystal stability[18] and to result in diffusivities that are much larger than those of typical solids. For simplicity, we will henceforth refer to such mesophase state as "solid" or ordered phase.

The rest of the paper is organized as follows. In Section 2, we explain our model, simulation methods, and analysis techniques, including the order parameters used to track the progress of the transition. In Section 3.1, we analyze what happens when the isotropic phase spontaneously transitions into the crystal phase, revealing that a significant portion of the isotropic phase has particles that are in a locally ordered configuration. In Section 3.2, we further characterize the phase transition using umbrella sampling (US) to determine the free-energy barriers associated with different degrees of metastability of the disordered phase. In Section 3.3, we describe a computer experiment intended to illustrate the ability of cubes to resolve grain boundary conflicts through co-operative rearrangements. Finally, in Section 4 we provide our concluding remarks.

2. METHODS

2.1. Model. For a given pair of cubes i and j, we use the hard pair potential given by

$$U_{ij} = \begin{cases} 0 & \text{if no overlap} \\ \infty & \text{if overlap} \end{cases} \tag{1}$$

The overlaps between any two cubes are detected using the separating axis theorem.[19]

2.2. Metropolis Monte Carlo (MC). Metropolis[6] Monte Carlo (MC) simulations were performed in an isothermal−isobaric (NPT) ensemble where the number of particles (N), the pressure, and the temperature of the system were kept constant. As per the conventions used in our previous studies,[8] the dimensionless pressure is $p = \beta p_a a_c^3$, where p_a is the actual unscaled pressure and a_c is the radius of the circumscribing sphere for a cube (for a cube of unit edge, it would be $\frac{\sqrt{3}}{2}$) and $\beta = 1/k_B T$ with k_B = Boltzmann constant. Simulations were conducted using periodic boundary conditions, and each MC cycle consisting of N translation, N rotation, and 2 isotropic volume moves. Each move was accepted based on the Metropolis acceptance criteria. For each pressure, at least 3×10^6 MC cycles were performed. All simulations were performed in a cubic box, and all system sizes had a perfect cube number of particles. For our ensuing discussions, we take the order−disorder phase transition of hard cubes to take place at $p = p_{co} = 4.0$ as estimated in the literature.[18] We note, however, that this value is only referential as the effective p_{co} in simulation will depend on system size, given the non-negligible finite-size effects known to particularly affect the ordered phase.[18]

2.3. Order Parameters. *2.3.1. q_4 Local Translational Order Parameter.* We use the q_4 Steinhardt[20,21] translational order parameter defined as follows: for every particle i, the local bond-order parameter, $q_{l,m}(i)$ is

$$q_{l,m}(i) = \frac{1}{N_b(i)} \sum_{j=1}^{l} Y_{l,m}(\theta_{i,j}, \phi_{i,j}) \tag{2}$$

where $N_b(i)$ is the number of neighbors of particle i, $Y_{l,m}(\theta, \phi)$ are the spherical harmonics, $\theta_{i,j}$ and $\phi_{i,j}$ are polar and azimuthal angles between particle i and its neighbor j, respectively, l is the symmetry index, and the value of m ranges from $-l$ to l. In this work, we use $l = 4$ to characterize cubatic order, henceforth using the symbol q_4 to refer to the collection of all 9 components ($2l + 1 = 9$). The neighbors of particle i are those particles whose centers of mass are within the cutoff distance $r_c = 1.4\sigma$ of particle i. The translational order correlation between particle i and its neighbor j, $d_q(i, j)$ is given by

DOI: 10.1021/acs.jpcb.8b06207
J. Phys. Chem. B 2018, 122, 9264−9273

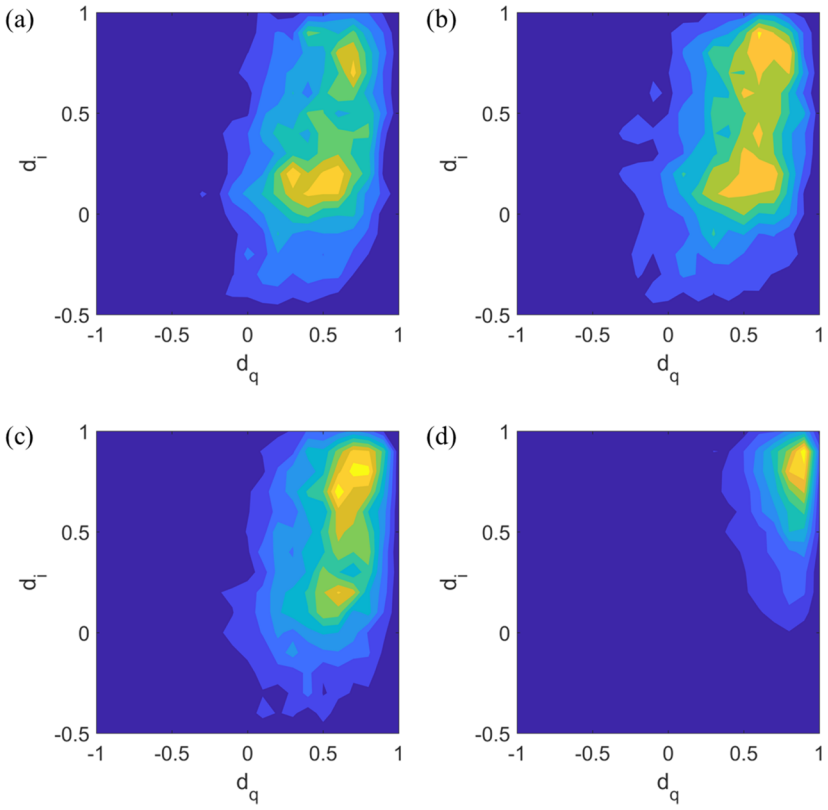

Figure 2. Contour plots for neighboring particle pair correlations, as the system transitions from disordered (a) to ordered (d) state. d_q captures the translational correlation and d_i the orientational correlation for a system of 1728 particles at $p = 4.07$. Frequency increases from blue to yellow. The equilibrium disordered phase (a) contains a non-negligible population of particles pairs that are near the same region of phase space that is frequented by the ordered state (d). The system transitions through stages (b, c) where the population of ordered pairs becomes more significant. In the ordered state, all particles populate the top-right corner (d).

$$d_q(i, j) = \frac{\sum_{m=-4}^{4} q_{4,m}(i) q_{4,m}^*(j)}{\left(\sum_{k=-4}^{4} |q_{4,k}(i)|^2\right)^{1/2} \left(\sum_{l=-4}^{4} |q_{4,l}(j)|^2\right)^{1/2}} \quad (3)$$

where the asterisk (*) denotes the complex conjugate.

2.3.2. i_4 Local Orientational Order Parameter. To study local orientational order, we use the i_4 order parameter[22] that captures the symmetry in orientations of cubes in the ordered phase. It is defined in a very similar manner as q_4, but instead of using the bond orientation vectors between two neighboring particles it uses the angles associated with individual particle axes orientations. In its normalized form, it is evaluated for a given particle j as

$$i_{4,m}(j) = \frac{\sum_{n=1}^{3} Y_{4,m}(\theta_n, \phi_n)}{\sqrt{\sum_{m=-4}^{4} \left|\sum_{n=1}^{3} Y_{4,m}(\theta_n, \phi_n)\right|^2}} \quad (4)$$

where $Y_{4,m}(\theta_n, \phi_n)$ are spherical harmonics with symmetry index 4 and θ_n and ϕ_n are polar and azimuthal angles of the three-particles axis n with respect to the reference coordinate frame. Analogous to translational order, the orientation correlation between two particles k and l is defined as

$$d_i(k, l) = \sum_{m=-4}^{4} i_{4,m}(k) . i_{4,m}^*(l) \quad (5)$$

where the asterisk (*) denotes complex conjugate. Although we primarily use d_i to detect local correlations of neighboring particles for most of our calculations, we also use it in Section 3.1 to obtain the orientation correlation function over distance, $d_i(r)$, which is the average value of $d_i(k, l)$ overall pairs of particles $\{k, l\}$ whose centers lie at a distance r from each other.

2.3.3. Labeling of Ordered Particles. The orientational order parameters i_4 and $d_i(k, l)$ are used to identify ordered particles; the rationale for this choice is discussed in the Section 3. Two particles k and l within the first neighbor cutoff distance $r_c = 1.4a$ are defined as connected if $d_i(k, l) > 0.7$. A particle with at least three connections is classified as ordered or solidlike. Solid clusters are identified by the condition that any two solidlike particles within r_c belong to the same cluster. The tunable parameters for the order parameters are set using criteria described in prior studies[15,23] for discriminating the disordered and ordered states; details on these calculations are provided in the Supporting Information (SI) (Figure S1).

2.3.4. P_4 Global Orientational Order Parameter. To obtain an overall measure of orientational order among N particles, we used global orientational order parameter, P_4 defined as

$$P_4 = \max_n \frac{3}{14N} \sum_i P_4(\mathbf{u}_i \cdot \mathbf{n}) = \max_n \frac{3}{14N} \sum_i (35 \cos^4 \theta_{i,n} - 30 \cos^2 \theta_{i,n} + 3) \quad (6)$$

where $\mathbf{u}_i$ is the unit vector along a relevant particle axis and $\mathbf{n}$ is a director unit vector which maximizes P_4 (see details in John et al.[24]) and $\theta_{i,n}$ is the angle contained by $\mathbf{u}_i$ and $\mathbf{n}$. The summation is performed overall three axes for all N particles. A value of $P_4 = 1$ describes perfect orientational order.

DOI: 10.1021/acs.jpcb.8b06207
J. Phys. Chem. B 2018, 122, 9264−9273

2.3.5. Particle Orientation Scatter Plot. Particle orientations can be visualized by plotting as dots on the surface of a unit sphere, the unit vectors corresponding to the orientation axes of all or a selected subset of particles in the system (see SI in Agarwal et al.).[8] The resulting plot reveals how correlated (clustered dots) or uncorrelated (diffused dots) those particle orientations are, e.g., in the perfect cubic crystal, all orientations will fall within six mutually orthogonal spots on the sphere, whereas in a fully isotropic phase the orientation dots will appear uniformly spread out over the whole spherical surface.

2.4. Umbrella Sampling (US). Umbrella sampling (US) simulations[15] were performed to determine free-energy barriers for the ordering transition. The total number of ordered particles ($N_{ordered}$) in the system was chosen to be a suitable reaction coordinate to describe the disorder−order transition, as preliminary results revealed that the solid phase did not emerge from a single nucleus, but rather from multiple regions in the entire system. The transition path along $N_{ordered}$ from the disordered to the ordered state was divided into overlapping equal-sized windows. The size of each window was varied depending on the conditions and the size of the system. Each window is simulated separately with reflective walls, and $N_{ordered}$ was recorded every 2 MC cycles. Reflective walls are implemented such that any trajectory leaving the window at the end of 2 MC cycles is returned to the configuration prior to those 2 MC cycles, which is counted again. Statistics obtained from each window are used to obtain relative free energies for the $N_{ordered}$ states within a window. Finally, individual sections are stitched together by matching values in the middle of the overlap between successive windows, keeping the value for the most frequent state in the disordered phase as the reference (zero point) for the calculation of the free-energy barrier ΔG^*, as described in earlier work.[15,16,25] Values of ΔG^* are scaled with respect to k_BT. We also implemented a version of US that allows mapping the free-energy surface over 2 order parameters despite using only a single-order parameter to bias or "drive" the simulations; this is done by concurrently book keeping a second "passenger" order parameter,[26] as further detailed in the SI (Figure S3).

2.5. Facet Alignment Measure. To quantify the degree of facet alignment between a pair of neighboring cubes i and j, the facet alignment measure $\Delta(i, j)$ introduced in an earlier study[16] was employed. In essence, Δ is the overlap area of the nearest interparticle facets (defined by the minimum centroid to centroid distance) when one is projected onto the other. This measure and its implementation have been described in detail in a previous study.[16]

3. RESULTS AND DISCUSSION

3.1. Spontaneous Phase Transition. Defining the degree of supersaturation (DSS) as the difference in chemical potentials between the isotropic and the solid phase,[13] the disorder-to-order first-order phase transition is spontaneous and the disordered phase metastable when DSS is positive. Such transitions are often characterized as following the mechanism of nucleation and growth[27,28] at low DSS (less than $2k_BT$[25]), eventually leading into a spinodal decomposition regime at very high supersaturation.[29] In this study, we are only considering cases where DSS is much less than $0.1k_BT$, for which a nucleation mechanism would be expected.

Upon compression of an isotropic system with stepwise pressure increments (starting with $p = 1$), we observe a spontaneous disorder-to-order transition at $p = 4.07$. The distribution of orientational and translational correlations is shown in Figure 2 as the transition progresses. It can be seen that the distributions of ordered and disordered particles are farther apart along d_i than along d_q, indicating that the orientational correlation is a better metric to discriminate between the two states. We observed that even at coexistence ($p = 4.0$), there is a non-negligible fraction of particles that are significantly more correlated than most particles in the disordered phase and experience a local environment that is akin to that of the ordered state. This amount of locally ordered particles is uncommon among polyhedral systems, for example, in case of octahedra[16] the population of such particles is comparatively small, as seen in Figure 3. Of course, any such comparison provides only a rough guide since the count of ordered particles depends on the order parameter used.

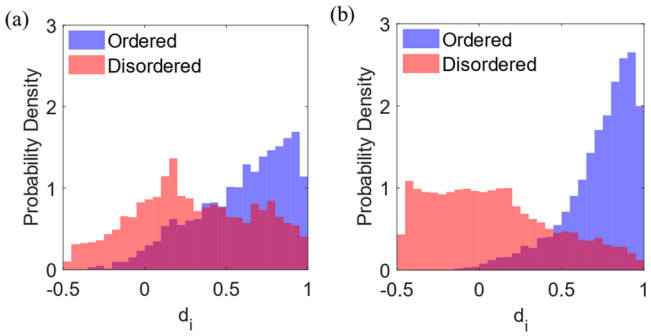

Figure 3. Orientational correlation distributions for (a) cubes and (b) octahedra[16] at liquid−solid coexistence conditions ($p_{co,cubes} \approx 4.0$, $p_{co,oct} \approx 6.93$). For cubes (octahedra), 65% (30%) of the particle population in the disordered phase has configurations occupying the same d_i region as the ordered phase.

We examined the spatial distribution of the locally ordered particles in the disordered phase to see if a large consolidated nucleus is distinguishable as the signature of a nucleation process as has been observed in other polyhedral particles.[15,16] Our clustering algorithm revealed that this is not the case; indeed, these particles were almost always sparsely distributed throughout the bulk disordered phase. For example, while about 4% of particles are ordered for $p_{co} = 4$, only $1/10^{th}$ of them are consolidated in the largest cluster. Even during the disorder-to-order transition, we observe that the increase in the total number of ordered particles precedes their consolidation into a single spanning cluster (Figure 4a). In the metastable isotropic basin, we observe that clusters of ordered particles are largely uncorrelated as shown in Figure 4b for a sample configuration and its corresponding spherical scatter plot for the orientation particle axes. As the transition progresses toward the ordered phase and 13% of the particles are ordered, we find that the clusters become more correlated, as evidenced in the scatter plot and snapshot of Figure 4c. In this case, we clearly see that the scatter plot has the characteristic symmetry with six orthogonal clusters. To further characterize this trend, we show in Figure 5 the distance-dependent orientational correlation function of the ordered particles, $d_i(r)$, during a transition at $p = 4.05$ for $N = 8000$ particles. When only 6% of the particles are ordered, the correlation decays to a very low value over a distance of $r \sim 10a_c$, revealing short-range order. For a 10.3% of ordered particles, which corresponds to the top of the free-energy barrier as discussed later in Section 3.2, the

DOI: 10.1021/acs.jpcb.8b06207
J. Phys. Chem. B 2018, 122, 9264−9273

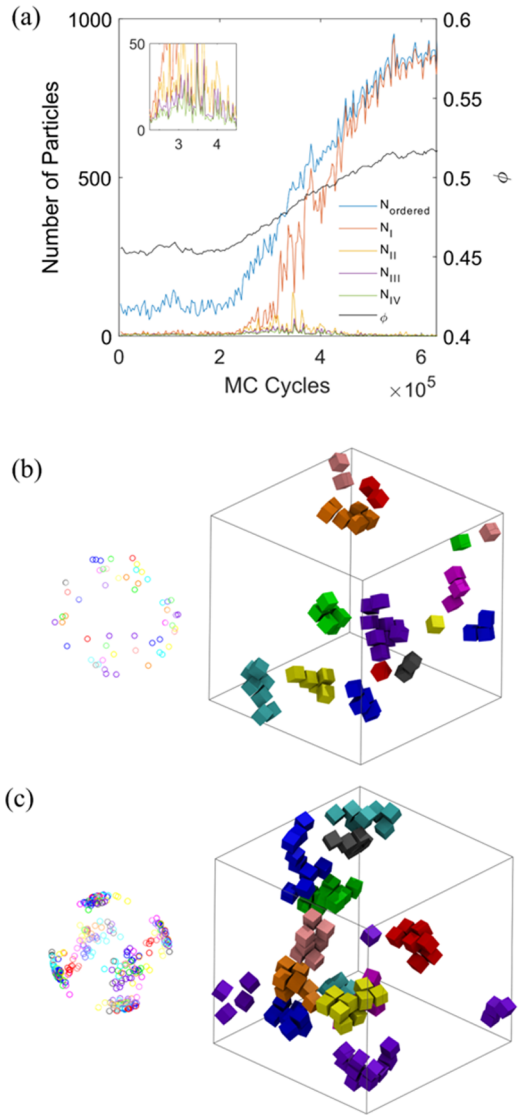

Figure 4. (a) Variation in number of ordered particles ($N_{ordered}$) and largest cluster sizes (N_I: largest, N_{II}: second largest, etc.) during a spontaneous transition at $p = 4.07$ and $N = 1728$. A steady increase in $N_{ordered}$ precedes a rise in the size of the largest cluster N_I (after 2×10^5 MC cycles). Before the consolidation, the relative size of various clusters is comparable (inset). ϕ (black line) is the volume fraction of the cubes. (b, c) Visualization of ordered particles at two points during the transition: when 6% ((b), 2.1×10^5 MC cycles) and 13% ((c), 2.1×10^5 MC cycles) of the particles are ordered. The 10 largest clusters are shown on the right, each with a different color that corresponds to those used in the scatter plot of particle orientation axes shown on the left.

particles become correlated over longer distances (i.e., across the simulation box length). This long-range correlation becomes even stronger as the fraction of ordered particles increases (i.e., to 13% as shown in Figure 5). Further, using an US calculation with the greatest cluster size as order parameter (which would be the appropriate reaction coordinate for a nucleation process) readily encounters multiple clusters of similar sizes coexisting in the system. This observation, which was common to simulations at all DSS values tested and for different definitions of solidlike particles making up the nuclei, indicates that the ordering process does not conform with the picture of classical nucleation. Hence, instead of the size of the

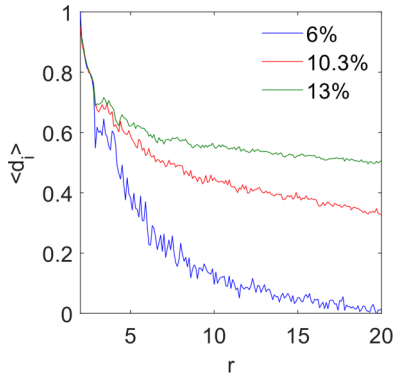

Figure 5. Mean d_i orientational correlation as a function of interparticle distance (r) for all of the ordered particles in a system at various percentages of ordered particles. Results for $p = 4.05$ and $N = 8000$ for cubes of side of two units of length.

largest consolidated nucleus, we chose the total number of ordered particles as an appropriate order parameter for this transition. Indeed, we find that such ordered particles occur spontaneously at a given pressure (see Figure 6), with their

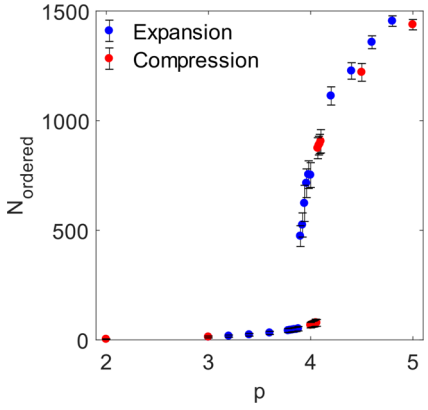

Figure 6. Number of spontaneously ordered particles ($N_{ordered}$) as a function of pressure (p) for a system of 1728 particles. Data points for compression from the isotropic phase in red and for expansion from the isotropic phase in blue. Error bars, representing 1 standard deviation from the mean, are shown as vertical bars on each point (as illustrated in the legend).

number increasing as the system's density slowly rises. For a $N = 1728$ system, compression from the isotropic state results in a sudden jump in $N_{ordered}$ at $p = 4.07$, while expansion from the ordered crystal results in a sharp drop in $N_{ordered}$ at $p = 3.90$. These results are only illustrative as the extent of hysteresis in the observable transition pressures around p_{co} depends on system size and the length of the simulation runs.

One contributing factor toward the presence of ordered domains in the disordered phase is the tendency of neighboring particles to align facets[16] (see Figure 7). Since the final-ordered structure has a very high population of facet-aligned particles compared to the disordered phase, it is expected that those local configurations in the latter with high facet alignment (high Δ values) would bear an imprint of the final-ordered structure. Since facet alignment is locally favored,[16] a local configuration that is disordered in d_i, but has a typical $\Delta \approx 0.5$ would be more likely to transition into an ordered configuration ($d_i > 0.75$, $\Delta > 0.7$). This is in contrast with the case of octahedra,[16] for which it was found that high-

DOI: 10.1021/acs.jpcb.8b06207
J. Phys. Chem. B 2018, 122, 9264−9273

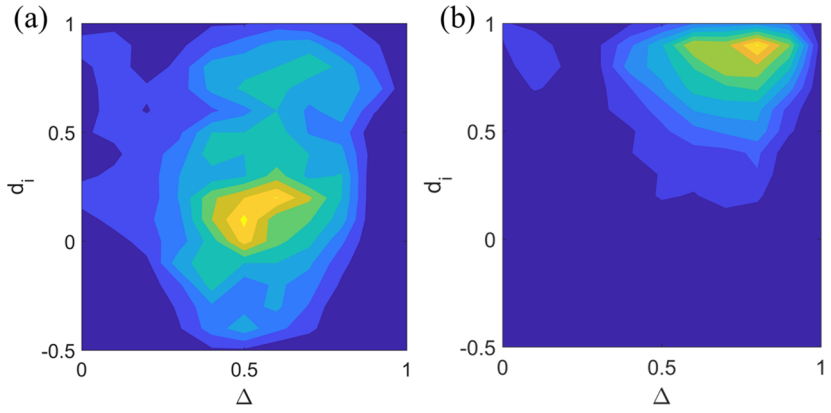

Figure 7. Contour plots describing the distribution of particle neighbor pairs over the orientational correlation (d_i) and facet alignment measure (Δ). The population moves toward a higher facet alignment as system goes from the disordered (a) to the ordered state (b). System of N = 1728 hard cubes at p = 4.

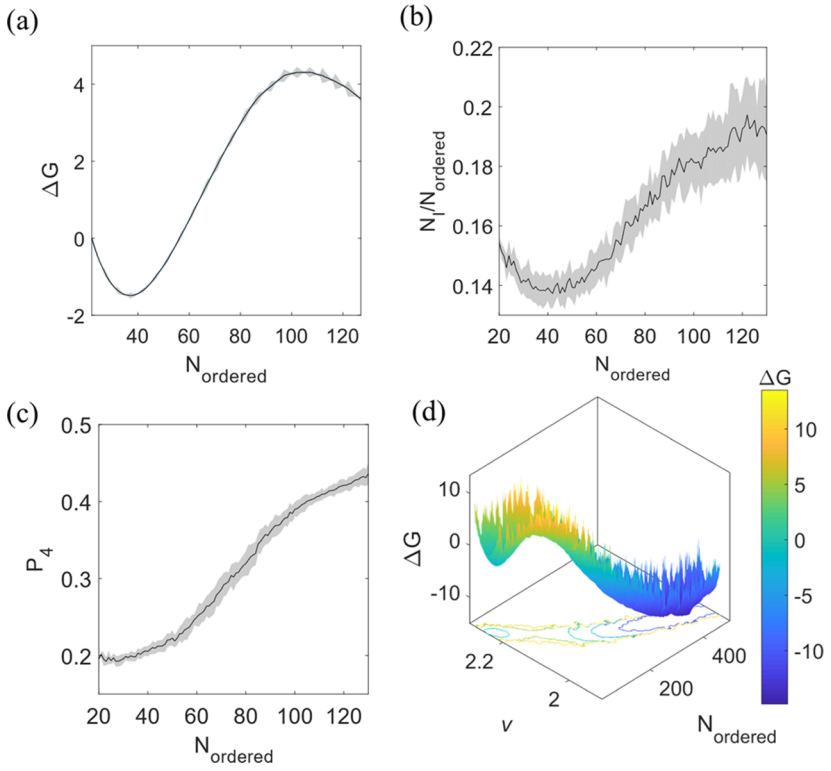

Figure 8. Umbrella sampling (US) calculations at p = 4 for N = 1000 particles. (a) ΔG profile along $N_{ordered}$; disordered-phase basin is centered around $N_{ordered}$ = 38. The top of the barrier corresponds to $N^*_{ordered}$ = 103. The gray shaded regions represent error bars from the US calculation. (b) Relative proportion of ordered particles present in the largest cluster, averaged over each US window. A minimum occurs for $N_{ordered} \in [30, 55]$, which precedes the inflexion point in (a) $N_{ordered} \sim 60$. (c) Global tetratic orientational order (P_4) for the ordered particles as the transition progresses, averaged over each US window. Orientational order increases more rapidly for $N_{ordered} \in [55, 103]$, likely due to the different ordered domains realigning as they merge. (d) Two-dimensional ΔG landscape with respect to $N_{ordered}$ and specific volume (v).

Δ disordered configurations hinder the ordering into the solid phase whose intrinsic low-Δ necessitates low-Δ configurations to precede the nucleation of translational order.

CNT is unsuitable to describe the present ordering transition as it neglects internuclei interactions and supposes bulk-average interfacial properties, assumptions that are inconsistent with the observed physical picture. Indeed, for all DSS values tested hard cubes order via multiple spontaneously forming and spatially interacting nuclei, whose small size and irregular, fluctuating shapes create effects that are not properly accounted for by just the bulk-average values of interfacial area and tension.

Thus, we hypothesized that at any given pressure above p_{co} an initially isotropic phase contains a certain fraction of particles forming multiple scattered ordered domains, which will increase as the ordering transition proceeds until such domains interact and consolidate. Such consolidation reduces the interfacial area and thus would be thermodynamically favored.

3.2. Free-Energy Barriers. Figure 8a shows the US results for the free-energy profile at p = 4 for a system of 1000

DOI: 10.1021/acs.jpcb.8b06207
J. Phys. Chem. B 2018, 122, 9264−9273

particles. We observe that there is a well-defined well within which the disordered phase exists with about 38 "ordered" particles (3.8% of total) present on average at a given time. Using US, we bias the system to explore rarer states with higher values of $N_{ordered}$. Eventually, we find that we attain a critical state, beyond which the system would be more likely[27] to spontaneously reach the ordered phase than the disordered phase. Figure 8b further shows that, overall, consolidation of the ordered domains increases with $N_{ordered}$. There exists, however, an initial decrease in the fraction of consolidated particles with $N_{ordered}$, indicating a regime where the ordered domains can grow while still being sufficiently dilute to avoid significant mutual interactions. Note that the $N_{ordered}$ value where the free-energy profile in Figure 8a has an inflexion point is close to where the minimum in Figure 8b occurs (i.e., $N_{ordered} \approx 55$). At this point additional ordered domains can be added to the system without any consolidation, which is unfavorable due to a concomitant increase in interfacial area. This is different from the behavior in the middle of the isotropic basin ($N_{ordered} = 38$) where the number of domains decreases with $N_{ordered}$. For $N_{ordered} > 55$, however, such merging of domains likely entails smaller changes in interfacial area so that the addition of newer domains leads to progressively smaller free-energy increments. Interestingly, we find that even as the orientational correlation P_4 (Figure 8c) among the ordered particles gradually increases with $N_{ordered}$, the increase is particularly rapid during this region of consolidation ($55 < N_{ordered} < 103$). Interestingly, at the top of the free-energy barrier ($N_{ordered} \approx 103$) less than 20% of all ordered particles have been consolidated into the largest cluster; the fact that the free energy decreases thereafter suggests that any further increase in $N_{ordered}$ involves a net reduction in interfacial area, i.e., consolidation reduces its value more than new ordered particles can increase it.

Since the system undergoes a significant change in specific volume (v) during the transition, we examined the relation between v and $N_{ordered}$ by concurrently obtaining statistics for v while mapping the free-energy landscape via US.[26] The resulting free-energy surface, shown in Figure 8d, reveals that $N_{ordered}$ and v are strongly correlated (within error bars, we obtained the same free-energy landscape when v is used as the primary order parameter in US, whereas $N_{ordered}$ is the passenger order parameter). We also performed another US simulation run in a reverse order (going from order to disorder) using the same $N_{ordered}$ as order parameter, and we found the that the free-energy barrier heights (from the disordered basin to the barrier top and from the ordered basin to the barrier top) were essentially the same as those found in the forward direction, indicating that this order parameter samples a reversible path across the transition. The values of the barriers determined from the two-dimensional free-energy surface of Figure 8d or from the one-dimensional free-energy profile of Figure 8a are nearly identical and thus we use the results from the latter approach for concreteness. The suitability of $N_{ordered}$ as order parameter for the transition-state region (around the free-energy barrier top) was further confirmed via the histogram test for the committor probability, as described in the SI (Figure S2).

To see whether the ordering transition is well described via a bulk phase property, we performed US calculations of the free-energy barrier ΔG^* for various system sizes using $N_{ordered}$ as order parameter. Figure 9 shows that for a given pressure, both properties scale linearly with system size N, and that the slope

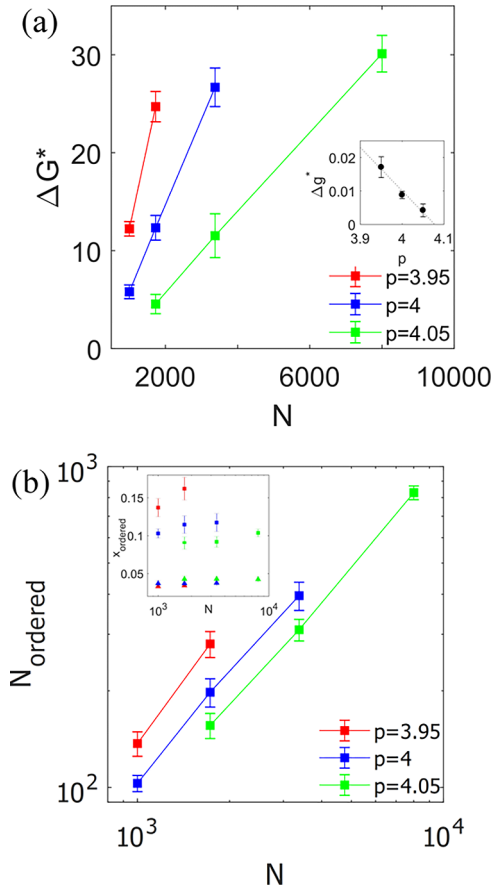

Figure 9. Free-energy barriers for the disorder-to-order transition at various pressures and system sizes (N). (a) Scaling of free-energy barrier (ΔG^*); the slope of the lines can be interpreted as an intensive free-energy barrier Δg^* which is shown in the inset for various pressures (p), along with a linear fit (dotted line). (b) Scaling of critical number of ordered particles. Inset: the fraction of ordered particles at the critical point ($x^*_{ordered}$, squares) and in the isotropic basin ($x^{iso}_{ordered}$, triangles); colors correspond to the pressures in the legend.

for a given pressure in Figure 9a, which would be equivalent to an "intensive" free-energy barrier Δg^* in Figure 9a, inset, and to a fraction of ordered particles $x^*_{ordered}$ in Figure 9b, inset, both remain nearly constant with N and decrease with pressure. Our hypothesis was that if the transition is a global or bulk process, both ΔG^* and the critical number of ordered particles ($N^*_{ordered}$) should scale linearly with respect to N (i.e., they would behave as "extensive" properties) with a prefactor that would be distinct from that expected for a nucleation process. Indeed, at the point when a classical nucleus of critical size N_c^* occurs, the total number of ordered particles in the system would be expected to follow a relation of the form

$$N^*_{ordered} = n^* N_c^* + x^{iso}_{ordered} N \quad (7)$$

where $x^{iso}_{ordered}$ is the fraction of ordered particles in the background, isotropic phase at the given DSS and n^* is the number of nuclei of size N_c^* in the system, which at equilibrium is given by $\sim N\, e^{-(\Delta G^*/k_B T)}$. Clearly, $n^* < 1$ for a large barrier (say $\Delta G^* > 10 k_B T$) and the system sizes used here $10^3 \le N < 10^4$, but $n^* = 1$ if a nucleus of size N_c^* is present. It follows then that for such nucleation scenario

DOI: 10.1021/acs.jpcb.8b06207
J. Phys. Chem. B 2018, 122, 9264−9273

$$x^*_{\text{ordered}} = N^*_{\text{ordered}}/N \sim x^{\text{iso}}_{\text{ordered}} \quad (8)$$

As shown in the inset of Figure 9b, $x^*_{\text{ordered}} \sim 0.1$, a value significantly larger than $x^{\text{iso}}_{\text{ordered}} \sim 0.04$ for the pressures considered, a disparity largely independent of N. Hence, although N^*_{ordered} would increase linearly with N even if the transformations were to proceed via nucleation, the calculated slope x^*_{ordered} is inconsistent with such an interpretation. Note that our results are also inconsistent with a linear percolation behavior where N^*_{ordered} would be proportional to $N^{1/3}$.

We note that as N increases at fixed p ($>p_{\text{co}}$) any long-range correlations that may have enhanced the stability of the ordered phase is weakened, leading to an increase in p_{co}, a reduction in $(p - p_{\text{co}})$ and DSS, and hence to an increase in ordering transition barrier ΔG^*. However, such finite-size effects are expected to be significant only for small system sizes $N < 10^3$ particles,[30] and be rather negligible for the range $10^3 \leq N < 10^4$ under consideration (and unlikely to lead to a linear scaling $\Delta G^* \propto N$). Note also that when the top of the free-energy barrier is reached most of our systems (~90%) are still in the isotropic phase where such finite-size effects are minimal. We hence argue that the linear scaling on N that we observe for N^*_{ordered} and ΔG^* are most consistent with a transition having a bulk-like behavior.

We further conjecture that the extrapolation of Δg^* to zero would mark a characteristic pressure (p_c) at which the ordering transition would be unrestricted (i.e., barrier-less). Our linear extrapolation (see Figure 9a, inset) indicates that $p_c \approx 4.08$, corresponding to DSS ≈ 0.03. From a physical point of view, $\Delta g^* > 0$ implies that in the large system limit (relevant to macroscopic experiments), the transition would be kinetically arrested. Only after the pressure is larger than a critical pressure (p_c) at which $\Delta g^* \leq 0$ can a spontaneous transition be kinetically viable. It should be pointed out, however, that our estimate of p_c is based on Δg^* values extrapolated from relatively small systems (Figure 9a) that neglect the potential contributions to the transition of density and ordering fluctuations occurring over lengths scales larger than the simulation box size, implying that $p_c \approx 4.08$ would be an overestimation.

The fact that cubes order via a process quite different from the nucleation mechanism that has been observed for other polyhedra (at comparable DSS),[14] including some from the truncated cube family,[15] could be traced to the unique characteristic of the mesophase-like solid that cubes form near the disorder−order transition (i.e., for $0.5 < \phi < 0.55$). As discussed in Section 1, such a solid phase could be seen as a mesophase not only because it contains an unusually large fraction of vacancies (~6.4%) for a crystal, but also because those vacancies are mobile and delocalized, spreading out over multiple lattice sites.[18] Indeed, the diffusivity of cubes is much larger than that of other polyhedra[8] or hard spheres in their solid states (near the ordering transition), which reflects the fast dynamics around the delocalized vacancies. The mobility of cubes in a solidlike cluster in contact with a disordered region is hence expected to be quite high and not too dissimilar to that of cubes in the disordered phase. The presence of "crystal" vacancies must amplify density fluctuations in a solid cluster and facilitate interfacial rearrangements, effects that may translate into a small interfacial tension. Indeed, the latter would in turn explain the tendency to form multiple metastable ordered clusters (rather than a single nucleus) during the ordering transition, despite the concomitant increase in interfacial area. Ultimately, the extensive nature of ΔG^* would largely arise from the fact that the interfacial area needed to consolidate the solid phase increases with system size.

3.3. Grain Boundary Dissolution. As shown in Figure 4a, at early stages of the ordering process we always observe the presence of multiple, independent ordered domains in the system, which if continued to grow without reorientation, would give rise to multiple grain boundaries. However, at least for the pressures and system sizes simulated, we never observe any (long-lived) polycrystallinity when the system fully transitions to the solid basin; the system always converges to a single-grain state. This ability to resolve domain misalignments likely plays a crucial role in facilitating the transition to the ordered phase. To gain some insight into the process of grain realignment, we created an artificial configuration consisting of two misaligned grains for $N = 5544$, as shown in Figure 10a. Grain 1 has particles with their faces aligned parallel to the box vectors, whereas grain 2 is rotated by 45° along the z-axis (pointing out of the page). We conducted NPT simulations at $p = 5$ and tracked the evolution of the merging process. We observe that as the system is equilibrated, grain 1 tends to propagate (Figure 10b). However, in the final structure (obtained after 6×10^6 MC cycles), both grains attain a final orientation that is intermediate between the original two orientations, albeit much closer to that of grain 1 (Figure 10c). Replicate simulations (not shown) exhibited a

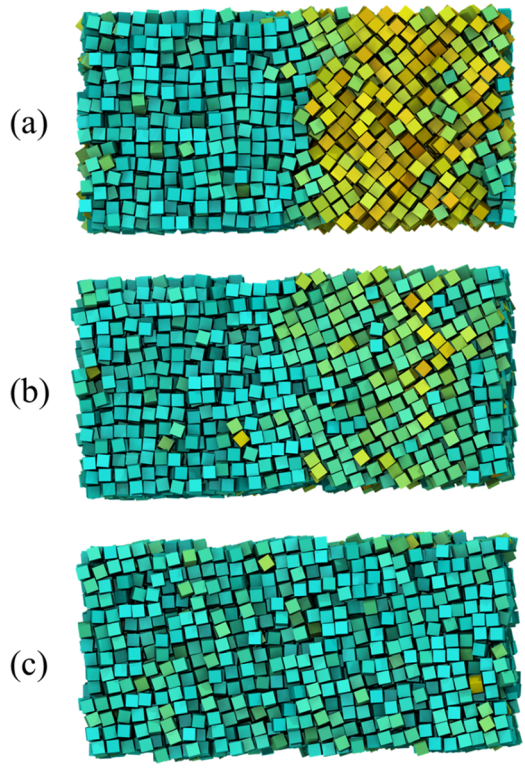

Figure 10. Dissolution of grain boundaries in hard cubes. (a) The initial system consists of two grains simulated at $p = 5$. Grain 2 (right) is rotated at 45° with respect to grain 1 (left), which is aligned with the simulation box axes. Cubes are colored based on their alignment: from blue for vertically aligned to yellow for 45° misalignment. (b) Grain 2 rotates driven by the facet alignment of particles at and around the grain boundaries. (c) Finally, the grains resolve into a single grain whose orientation is close to that of the original grain 1.

DOI: 10.1021/acs.jpcb.8b06207
J. Phys. Chem. B 2018, 122, 9264−9273

similar behavior, with the final orientation being intermediate, with varying proximity to the original orientation of either grain 1 or grain 2. If disparate-sized grains were to meet, the smaller grain would likely consistently experience the largest reorientation. The process is vaguely reminiscent of Ostwald ripening, wherein one grain grows by the gradual dissolution and particle transfer from another grain, except that in this case the grains are not dispersed in a solution and can hence "push" against each other. This capability of hard cubes to reorganize quickly, even when large grains are involved (as in this example) helps explain the absence of polycrystallinity in the ordered phase, as multiple ordered domains would be able to conveniently merge. Once again, the high concentration of delocalized (dynamic) vacancies[18] and the high particle mobility[8] unique to hard cubes' solid-phase provide the likely microscopic mechanisms that facilitate the co-operative rearrangement of particles near an interface and the propagation of those changes through the grains. Indeed, Smallenburg et al.[18] found that spontaneous vacancies account for up to 6.4% (of lattice sites), which is several orders of magnitude larger than typically seen in colloidal crystals, including octahedra for which vacancies would not be observed in typical simulation system sizes (unless purposely implanted, in which case they would have minimal mobility).

4. CONCLUSIONS

Our analysis of the disorder-to-order phase transition of hard cubes reveals that due to high level of local facet alignment occurring in both the ordered phase and (to a lesser extent) in the disordered phase, there is a high propensity in the latter to contain small ordered domains. At any given time, such domains are present in non-negligible quantities, such that the total number of ordered particles describes the proximity to the ordered phase better than the size of the largest cluster alone. Analysis of unbiased simulations reveals that the transition involves an increase in the number of such domains, followed by their consolidation. Umbrella sampling calculations reveal that the free-energy transition barriers obtained from systems of different sizes are consistent with the view that the transition happens via a bulk process. Calculation of an intensive free-energy barrier allows us to extrapolate to a critical pressure p_c above which the transition in a macroscopic system would take place unhindered and spontaneously. The absence of polycrystallinity in the solid phase is linked to the ability of the system to dissolve grain boundaries via co-operative, correlated motions that propagate through the grains as demonstrated by the simulation of misaligned grains that realigned by simultaneously changing their original orientations. Indeed, ordered domains that spontaneously arise and come in contact during the disorder-to-order process readily resolve any grain boundaries, resulting in a final single-grain ordered phase.

The existence of such a global ordering mechanism for hard cubes brings up the question about what other systems might exhibit a similar mechanism. Clearly, truncated cubes with a small amount of truncation[13] or rounded cubes (described via superball[31] or polybead models[22]) which undergo a similar transition into a cubic ordered phase should closely approach the behavior of the hard cubes studied here. More generally, systems with a strong coherence in their tendencies for local packing (in disordered phase) and global packing (in ordered phase) may exhibit a similar mechanism. For practical applications, it would be of interest to quantify the effect on the ordering mechanism of soft interparticle attractions[21] and size polydispersity,[30] two factors which are ubiquitous in experimental systems. Further studies can focus on finding theoretical models that can describe the general features of the phase-transition mechanism studied here, incorporating the key elements that we observed in hard cubes, such as a high concentration of locally ordered particles in the isotropic phase basin and the proliferation and consolidation of ordered domains before reaching the solid-phase basin. Also, studies employing methods designed to sample the disorder-to-order transition kinetics and rates[14,28] would provide complementary insights into the microstructure changes along transition pathways.

■ ASSOCIATED CONTENT

Supporting Information

The Supporting Information is available free of charge on the ACS Publications website at DOI: 10.1021/acs.jpcb.8b06207.

Further discussion on order parameter optimization and umbrella sampling methodology (PDF)

■ AUTHOR INFORMATION

Corresponding Author

*E-mail: fe13@cornell.edu.

ORCID

Fernando A. Escobedo: 0000-0002-4722-9836

Notes

The authors declare no competing financial interest.

■ ACKNOWLEDGMENTS

Funding supports from NSF awards DMR-1609997 and CBET-1402117 are gratefully acknowledged. The authors are grateful to Dr. Vikram Thapar for valuable discussions and sharing the base simulation code.

■ REFERENCES

(1) Whitesides, G. M.; Grzybowski, B. Self-Assembly at All Scales. *Science* **2002**, *295*, 2418−2421.

(2) Manoharan, V. N. Colloidal Matter: Packing, Geometry, and Entropy. *Science* **2015**, *349*, No. 1253751.

(3) Cademartiri, L.; Bishop, K. J. M. Programmable Self-Assembly. *Nat. Mater.* **2015**, *14*, 2−9.

(4) Zeravcic, Z.; Manoharan, V. N.; Brenner, M. P. Colloquium: Toward Living Matter with Colloidal Particles. *Rev. Mod. Phys.* **2017**, *89*, 1−14.

(5) Frenkel, D. Order Through Entropy. *Nat. Mater.* **2015**, *14*, 9−12.

(6) Metropolis, N.; Rosenbluth, A. W.; Rosenbluth, M. N.; Teller, A. H.; Teller, E. Equations of State Calculations by Fast Computing Machine. *J. Chem. Phys.* **1953**, *21*, 1087−1092.

(7) Onsager, L. The Effects of Shape On The Interaction Of Colloidal Particles. *Ann. N. Y. Acad. Sci.* **1949**, *51*, 627−659.

(8) Agarwal, U.; Escobedo, F. A. Mesophase Behaviour of Polyhedral Particles. *Nat. Mater.* **2011**, *10*, 230−235.

(9) Henzie, J.; Grünwald, M.; Widmer-Cooper, A.; Geissler, P. L.; Yang, P. Self-Assembly of Uniform Polyhedral Silver Nanocrystals into Densest Packings and Exotic Superlattices. *Nat. Mater.* **2011**, *11*, 131−137.

(10) Gantapara, A. P.; De Graaf, J.; Van Roij, R.; Dijkstra, M. Phase Diagram and Structural Diversity of a Family of Truncated Cubes: Degenerate Close-Packed Structures and Vacancy-Rich States. *Phys. Rev. Lett.* **2013**, *111*, No. 015501.

DOI: 10.1021/acs.jpcb.8b06207
J. Phys. Chem. B 2018, 122, 9264−9273

(11) Damasceno, P. F.; Engel, M.; Glotzer, S. C. Predictive Self-Assembly of Polyhedra into Complex Structures. *Science* **2012**, *337*, 453−457.
(12) Auer, S.; Frenkel, D. Prediction of Absolute Crystal-Nucleation Rate in Hard-Sphere Colloids. *Nature* **2001**, *409*, 1020−1023.
(13) Auer, S.; Frenkel, D. Numerical Prediction of Absolute Crystallization Rates in Hard-Sphere Colloids. *J. Chem. Phys.* **2004**, *120*, 3015−3029.
(14) Gantapara, A. P.; De Graaf, J.; Van Roij, R.; Dijkstra, M. Phase Behavior of a Family of Truncated Hard Cubes. *J. Chem. Phys.* **2015**, *142*, No. 054904.
(15) Thapar, V.; Escobedo, F. A. Localized Orientational Order Chaperones the Nucleation of Rotator Phases in Hard Polyhedral Particles. *Phys. Rev. Lett.* **2014**, *112*, No. 048301.
(16) Sharma, A. K.; Thapar, V.; Escobedo, F. Solid-Phase Nucleation Free-Energy Barriers in Truncated Cubes: Interplay of Localized Orientational Order and Facet Alignment. *Soft Matter* **2018**, *14*, 1996−2005.
(17) van Anders, G.; Klotsa, D.; Ahmed, N. K.; Engel, M.; Glotzer, S. C. Understanding Shape Entropy through Local Dense Packing. *Proc. Natl. Acad. Sci. U.S.A.* **2014**, *111*, E4812−E4821.
(18) Smallenburg, F.; Filion, L.; Marechal, M.; Dijkstra, M. Vacancy-Stabilized Crystalline Order in Hard Cubes. *Proc. Natl. Acad. Sci. U.S.A.* **2012**, *109*, 17886−17890.
(19) Gottschalk, S.; Lin, M. C.; Manocha, D. OBB Tree: A Hierarchical Structure for Rapid Interference Detection. In *Proceedings of SIGGRAPH 96*, 1996; pp 171−180.
(20) Steinhardt, P.; Nelson, D.; Ronchetti, M. Bond-Orientational Order in Liquids and Glasses. *Phys. Rev. B* **1983**, *28*, 784−805.
(21) Rein ten Wolde, P.; Ruiz-Montero, M. J.; Frenkel, D. Numerical Calculation of the Rate of Crystal Nucleation in a Lennard-Jones System at Moderate Undercooling. *J. Chem. Phys.* **1996**, *104*, 9932−9947.
(22) Escobedo, F. A. Effect of Inter-Species Selective Interactions on the Thermodynamics and Nucleation Free-Energy Barriers of a Tessellating Polyhedral Compound. *J. Chem. Phys.* **2016**, *145*, No. 211903.
(23) Filion, L.; Hermes, M.; Ni, R.; Dijkstra, M. Crystal Nucleation of Hard Spheres Using Molecular Dynamics, Umbrella Sampling, and Forward Flux Sampling: A Comparison of Simulation Techniques. *J. Chem. Phys.* **2010**, *133*, No. 244115.
(24) John, B. S.; Juhlin, C.; Escobedo, F. A. Phase Behavior of Colloidal Hard Perfect Tetragonal Parallelepipeds. *J. Chem. Phys.* **2008**, *128*, No. 044909.
(25) Sharma, A. K.; Escobedo, F. A. Nucleus-Size Pinning for Determination of Nucleation Free-Energy Barriers and Nucleus Geometry. *J. Chem. Phys.* **2018**, *148*, No. 184104.
(26) Meadley, S. L.; Escobedo, F. A. Thermodynamics and Kinetics of Bubble Nucleation: Simulation Methodology. *J. Chem. Phys.* **2012**, *137*, No. 074109.
(27) White, G. M. Steady-State Random Walks with Application to Homogeneous Nucleation. *J. Chem. Phys.* **1969**, *50*, 4672.
(28) Kashchiev, D. Forms and Applications of the Nucleation Theorem. *J. Chem. Phys.* **2006**, *125*, No. 014502.
(29) Trudu, F.; Donadio, D.; Parrinello, M. Freezing of a Lennard-Jones Fluid: From Nucleation to Spinodal Regime. *Phys. Rev. Lett.* **2006**, *97*, No. 105701.
(30) Frenkel, D.; Smit, B. *Understanding Molecular Simulations: From Algorithms to Applications*; Academic Press, 2002.
(31) Ni, R.; Gantapara, A. P.; de Graaf, J.; van Roij, R.; Dijkstra, M. Phase Diagram of Colloidal Hard Superballs: From Cubes via Spheres to Octahedra. *Soft Matter* **2012**, *8*, 8826.

DOI: 10.1021/acs.jpcb.8b06207
J. Phys. Chem. B 2018, 122, 9264−9273